

# Properties of High Redshift Galaxies

D. Calzetti

*Space Telescope Science Institute, 3700 San Martin Drive, Baltimore, MD 21218, U.S.A.*

## Abstract

I review the characteristics of high redshift galaxies, with particular attention to the effects of dust obscuration on the observed light. Galaxies at redshift  $z \sim 1$  and at  $z > 2$  are discussed separately, as the accessible information for each redshift range are different. In the  $z \leq 1-2$  redshift region, data on the  $H\alpha$  and mid/far-IR luminosity of the galaxies are becoming increasingly available, effectively complementing the restframe UV data; they offer a better handle on the amount of dust obscuration present in the galaxies, although some ambiguity remains as to the distribution of the dust within the system and the opacity correction factor this implies. At higher redshifts, most of the available data cover the far-UV region only, representing a challenge for a careful assessment of the effects of dust in galaxies. Finally, I discuss the implications of the dust corrections to the star formation rate density of the Universe as a function of redshift.

## 1 Introduction

The study of galaxy populations at high redshift is aimed at understanding how galaxies evolved into their low-redshift counterparts. One of the tools for achieving this goal is the investigation of the stellar populations, their evolution, and their relation to the galaxy morphological type, via the observation and analysis of the emitted light.

Current instrumentation provides most immediate access to the optical and near-IR part of the electromagnetic spectrum, which correspond to restframe UV and optical wavelengths for redshifts  $z \geq 1$ . The availability of restframe UV measurements is particularly important for quantifying the evolution of the star formation rate in galaxies (Lilly et al. 1996, Madau et al 1996). Newly formed massive stars emit the bulk of their energy in the UV (e.g., Leitherer & Heckman 1995), and light in this waveband is a sensitive indicator of recent star formation, over timescales of  $\sim 100$  Myr. Measuring the evolution of the star formation is a direct way to measure the evolution of the stellar populations in a galaxy.

The UV emission from a galaxy is, however, heavily affected by the presence of even small quantities of dust. Sources which are optically thin in the visible (e.g.,  $A_V = 0.3$ ) can be optically thick in the UV ( $A_{1300\text{\AA}} \simeq 1$ ). Light at longer wavelengths is progressively less sensitive to the effects of dust obscuration, but also less sensitive to recent star formation (if we exclude the Red Supergiants in the near-IR). Exception to this rule are the nebular emission lines (e.g.,  $H\beta$ ,  $H\alpha$ , [OII], etc.), which are directly excited by ionizing photons, and the emission from dust at wavelengths  $\geq 30 \mu\text{m}$ . Redshifted nebular emission lines fall in the near/mid-IR wavelength range; for instance, the bluest of the strong emission lines, [OII]( $\lambda 3727 \text{\AA}$ ) is redshifted to  $1.1 \mu\text{m}$  in a  $z=2$  galaxy. The detection and measurement of emission lines in high redshift

galaxies is rather difficult at present because of the limited sensitivity of near-IR and mid-IR instrumentation (see, however, the results of Pettini et al. 1998, Glazebrook et al. 1999, Yan et al. 1999). Dust heated by hot stars to temperatures  $T \geq 30$  K emits in the far-IR and represents an indirect, but sensitive, indicator of star formation in a galaxy (e.g., Helou 1986, Young et al. 1989); in addition, it is, by definition, insensitive to dust obscuration. Recent far-IR and sub-mm instruments, like ISO and SCUBA, have reached high enough sensitivities to be able to measure dust emission from distant galaxies. There are, nevertheless, residual problems with this type of measures: limitations by source confusion, uncertainties in source positioning which hamper the assignment of optical counterparts and, therefore, of redshifts to the dust-emitting sources, possibility of AGN contamination, and uncertainties in the dust spectral energy distribution (SED) represent difficulties which have not been completely overcome yet (see, however, Barger et al. 1999). The latter of these problems is briefly discussed in section 3 below.

In this talk I concentrate on the UV and optical properties of galaxies at redshift  $z \geq 1$ , and the effects of dust obscuration on the emerging light. Galaxies at  $z \leq 1$  are discussed in another contribution to these Proceedings (see, F. Hammer), while the characteristics of medium-high redshift galaxy populations detected in the far-IR and sub-mm are presented by S. Lilly, D. Hughes, J.-L. Puget and others (also these Proceedings).

## 2 Galaxies at Redshift $z \sim 1$

The restframe UV luminosity density of galaxies displays a five/ten-fold increase from  $z \sim 0$  to  $z \sim 1$  (Lilly et al. 1996). This result has been interpreted as a comparable increase in the star formation rate density (SFRD) of the Universe with redshift (Madau et al. 1996, and subsequent papers). Galaxies were therefore forming stars at a higher pace about 9 Gyr ago than today, roughly the same trend expected in CDM galaxy evolution models (e.g., Baugh et al. 1998). Although the observed trend is probably correct, the actual numbers for the absolute value and the slope of the SFRD- $z$  relation derived from the restframe UV data needed independent confirmation, because UV measurements are potentially affected by dust obscuration. Nevertheless, it is likely that the intrinsic SFRD between  $z=0$  and  $z=1$  is at most a factor  $\sim 3$ – $3.5$  higher than what derived from the UV measurements; larger values of the SFRDs would make galaxies quickly run out of gas, under most assumptions for the stellar IMF and for the gas recycling from supernovae and massive stars (Calzetti & Heckman 1999; Pei, Fall & Hauser 1999). Recent ISO 15  $\mu\text{m}$  observations of the galaxies in the Lilly et al. fields confirm the large increase of the SFRD with redshift in the range 0.3–1, but also show that the absolute value of the SFRD can be as much as  $\sim 3$  times higher than that measured from the UV data (Flores et al. 1999, see also Hammer, this Conference). Still, we should bear in mind that the derivation of the SFRD from the ISO data is somewhat uncertain, as the extrapolation from the restframe  $\sim 10 \mu\text{m}$  flux density to the bolometric far-IR dust emission is a non-trivial step.

Galaxies at  $z \leq 1$ – $1.5$  can be tested for the presence of dust obscuration by complementing the UV data with measurements at redder wavelengths of, e.g., nebular emission lines, like  $\text{H}\alpha$ , which are excited by young massive ionizing stars, but are also less sensitive to the effects of dust. Technically, this method only tests for *dust reddening*, not dust obscuration, because regions which are opaque at  $\sim 7000 \text{ \AA}$  will not be detected in either UV or  $\text{H}\alpha$ . Glazebrook et al. (1999) and Yan et al. (1999) measured the  $\text{H}\alpha$  emission from galaxies at redshift  $z \approx 1$ . In both cases it is found that the average SFR derived from  $\text{H}\alpha$ ,  $\text{SFR}(\text{H}\alpha)$ , is systematically higher than the average SFR derived from the restframe UV emission at  $2800 \text{ \AA}$ ,  $\text{SFR}(2800)$ .

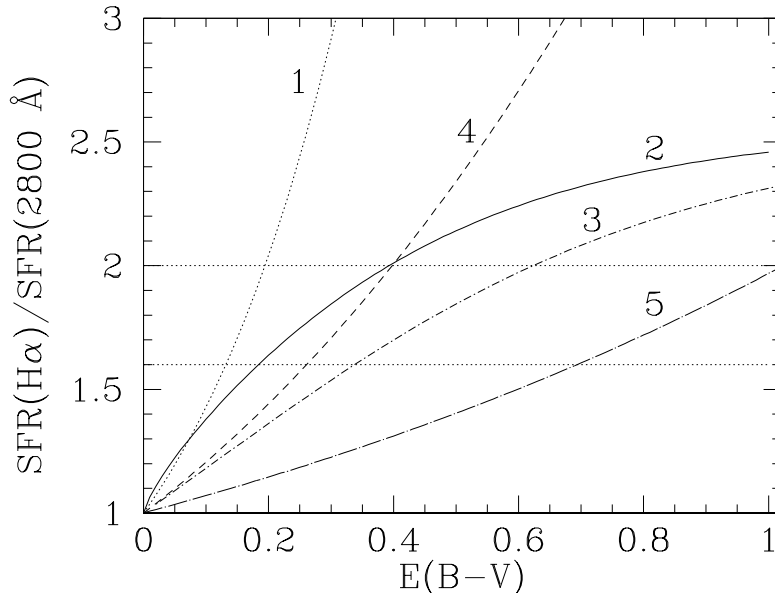


Figure 1: The ratio of the star formation rates measured from the **observed**  $H\alpha$  line emission and from the UV continuum emission at  $2800 \text{ \AA}$ ,  $SFR(H\alpha)/SFR(2800)$ , plotted as a function of the mean galaxy color excess  $E(B-V)$ , for 5 different dust geometry models: 1. homogeneous, foreground screen; 2. homogeneous disk; 3. homogeneous spheroid; 4. clumpy shell; 5. starburst dust distribution (see text for explanations on the different models). The horizontal lines mark approximately the range given by the observational data (equation 1).

In particular:

$$\frac{SFR(H\alpha)}{SFR(2800)} \sim 1.6 - 2, \quad (1)$$

(with fairly large error bars). In the absence of dust obscuration,  $SFR(H\alpha)/SFR(2800)=1$ , where reference SFRs are derived from models of stellar populations with constant star formation since 1 Gyr and a standard Salpeter stellar IMF (Glazebrook et al. 1999). A value  $>1$  in equation 1 is expected if the emerging light is attenuated by dust. It is to be remarked that the  $H\alpha$  line emission and the UV continuum emission at  $2800 \text{ \AA}$  are sensitive to *different* star formation timescales:  $H\alpha$  probes only the most recent star formation, being produced only when the short-lived ionizing stars are present (timescales of  $\sim 10$  Myr); the UV emission at  $2800 \text{ \AA}$  is contributed also by long-lived, non-ionizing stars, and measures star formation over timescales of  $\sim 100$ – $500$  Myr. Therefore, if the adopted model for the stellar population does not match reality, the intrinsic value of the ratio  $SFR(H\alpha)/SFR(2800)$  can change by as much as  $\sim 30$ – $60\%$ ; for a population younger than  $\sim 1$  Gyr, the change goes in the direction of decreasing the ratio of equation 1, implying lower dust attenuations. For sake of simplicity, I assume in the following that a 1 Gyr constant star formation stellar population is a fair representation of a  $z\sim 1$  galaxy.

Establishing that the  $z\sim 1$  galaxies are affected by dust reddening is far more straightforward than measuring *the amount of dust reddening* itself. This measurement involves making assumptions on the distribution of the dust inside the galaxy, and quite different results can be obtained for different dust geometries (Witt, Thronson & Capuano 1992, Calzetti, Kinney & Storchi-Bergmann 1994). Examples are shown in Figures 1 and 2. In these figures, five simple models for the geometry of dust in galaxies are used to derive the observed  $SFR(H\alpha)/SFR(2800)$  and the fraction of light emerging in the UV continuum and in the  $H\alpha$  line as a function of the dust optical depth, here given as color excess  $E(B-V)$ . The first model is the standard homogeneous, foreground dust screen, frequently used to derive dust reddening in galaxies (e.g.,

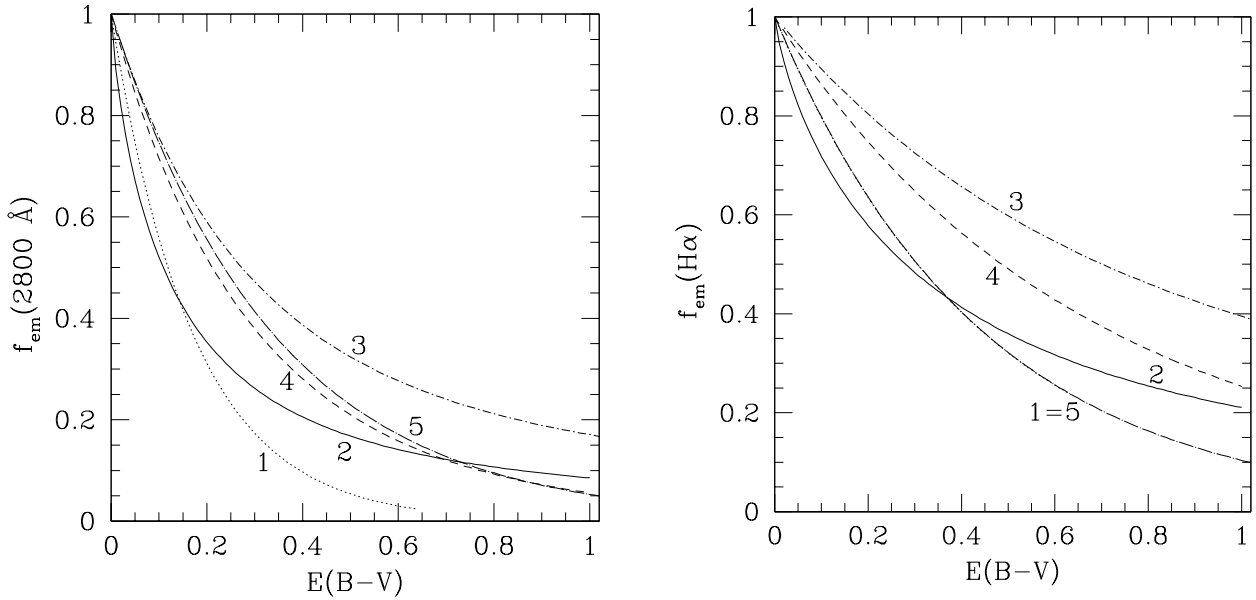


Figure 2: The fraction of emerging light in the UV continuum (left panel) and in the  $H\alpha$  line (right panel) as a function of increasing mean galaxy color excess  $E(B-V)$ . The numbering of the five dust models used to derive  $f_{em}$  follows the same convention as Figure 1.

Glazebrook et al. 1999, Yan et al. 1999); this model is an extreme case under most assumptions, since it implies not only that all the dust is completely foreground to all the stars in the galaxy, but also that the dust screen is far away enough from the galaxy that scattering of light into the line of sight is a negligible effect (e.g., Calzetti et al. 1994). In the second model the dust and the stars are homogeneously mixed together and are distributed in a flattened disk (homogeneous disk); the case shown in Figures 1 and 2 assumes that the opacity is averaged over all possible inclination angles of the disks. The third model is also an homogeneous mixture of dust and stars, but the two are distributed in a sphere (homogeneous spheroid). In the fourth model, the stars are centrally concentrated, while the dust is clumpy and located in a shell surrounding the stars (clumpy shell). The fifth model uses the distribution of dust and stars typically found in starburst galaxies at low redshift (Calzetti et al. 1994, Calzetti 1997a, Calzetti et al. 1999); here the distribution of the dust is roughly equivalent to a clumpy shell (Gordon, Calzetti & Witt 1997), except that the ionized gas is on average twice as attenuated as the stellar continuum (Calzetti et al. 1994).

Figure 1 shows that the same value of  $SFR(H\alpha)/SFR(2800)$  corresponds to rather different values of the color excess in different dust models. For instance, for the homogeneous disk (model 2),  $SFR(H\alpha)/SFR(2800)=2$  implies  $E(B-V)=0.4$ , with 21% and 41% of the UV and  $H\alpha$  light, respectively, emerging from the galaxy. For the starburst dust distribution (model 5), the same SFR ratio implies  $E(B-V)=1.0$  and 5% and 10% of the UV and  $H\alpha$  light, respectively, emerging from the galaxy.

If we exclude the homogeneous screen model, the observed range of  $SFR(H\alpha)/SFR(2800)$  implies correction factors between 2.3 and 5 for the UV light at  $2800 \text{ \AA}$  and between 1.4 and 2.4 for the  $H\alpha$  line, for models 2 through 4. A more extreme situation is represented by the starburst reddening model, where only between 5% and 13% of the UV light and between 10% and 21% of the  $H\alpha$  light emerge from the galaxy. This extreme behavior is due to the differential reddening between ionized gas and stellar continuum. A dust correction factor 10 or so for the observed UV flux density would give, however, an excessively high value of the intrinsic SFRD at  $z \approx 1$ , probably high enough to deplete galaxies of their gas content before  $z=0$ . Thus, the starburst model does not appear applicable to the  $z \sim 1$  galaxies; this is expected

for systems older than a few Gyrs, which have evolved beyond their initial few generations of stars, and whose emission is not dominated by a central starburst.

The basic conclusion is that, if the values of equation 1 are confirmed by further observations, the intrinsic SFRD at  $z \sim 1$  is more than a factor 2 and likely less than a factor 5 larger than what directly inferred from the observed UV flux density.

### 3 Galaxies at Redshift $z > 2$

The population of galaxies at  $z > 2-2.5$  identified with the Lyman-break technique (Steidel et al. 1996) show observational characteristics similar to those of the central regions of local UV-bright starburst galaxies. In both cases the objects are active star-forming systems with observed SFRs per unit area of  $\approx 1 M_{\odot} \text{ yr}^{-1} \text{ kpc}^{-2}$  (Calzetti & Heckman 1999, Meurer et al. 1997). Restframe UV spectra, which generally cover the range 900–1800 Å, show a wealth of absorption features, and sometimes P-Cygni profiles in the CIV(1550 Å) line (cf. the figures in Steidel et al. 1996), typical of the predominance of young, massive stars. Restframe optical spectra available for a few Lyman-break galaxies (Pettini et al. 1998) show nebular emission lines with the typical intensities seen in local starbursts (Meurer, Heckman, & Calzetti 1999).

Another characteristic the two populations share is the large spread in restframe UV colors (e.g., Dickinson 1998). If the observed UV stellar continuum is parametrized by a power law,  $F(\lambda) \propto \lambda^{\beta}$ , in the range  $\sim 1200-1800$  Å, Lyman-break galaxies cover a large range of  $\beta$  values, roughly from  $-3$  to  $0.4$ , namely from very blue to moderately red (Dickinson 1999, private communication). This range is not very different from that covered by the local, UV-bright starbursts. Population synthesis models (e.g. Leitherer & Heckman 1995) indicate that a dust-free, young starburst or constant star-formation population have invariably values of  $\beta < -2.0$ , for a vast range of metallicities. For the local starbursts, the most straightforward interpretation for the observed range of UV spectral indices is dust reddening (Calzetti et al. 1994). Dust reddening has been proposed as an explanation also in the case of the Lyman-break galaxies (Calzetti 1997b, Meurer et al. 1997, 1999, Pettini et al. 1998, Steidel et al. 1999). The observed UV emission from the galaxies at  $z \sim 3$  then accounts, on average, for  $\sim 20-25\%$  of the intrinsic UV luminosity (Steidel et al. 1999). Similar fractions of observed-to-intrinsic UV luminosity are expected in evolution models of the dust content of galaxies (Calzetti & Heckman 1999, Pei et al. 1999).

If the interpretation of the high- $z$  UV color spread is correct, the light absorbed by dust at UV–optical wavelengths should appear in the far-IR as dust emission. As already discussed in the previous section for UV and  $H\alpha$ , the UV slope  $\beta$  technically measures dust reddening, not dust obscuration; i.e., UV light from stars deeply buried inside dust does not contribute, in principle, to the UV emission and slope (Calzetti et al. 1995). Meurer et al. (1999) tested the relation between reddening and obscuration in local starburst galaxies by comparing  $\beta$  with  $FIR_{IRAS}/F(UV)$ ; this ratio is a measure of total dust obscuration because  $FIR_{IRAS}$  and  $F(UV)$  have roughly opposite trends for increasing amounts of dust ( $FIR_{IRAS}$  increases while  $F(UV)$  tends to decrease), while they are both proportional to the SFR of the galaxy. Calzetti et al. (1999) use recent ISO observations of local starbursts to directly compare the amount of energy emitted by dust in the far-IR with predictions for the energy absorbed by dust in the UV–optical; the latter quantity is derived using the reddening recipe of Calzetti et al. (1994) and Calzetti (1997b). The basic conclusion is that reddening and total obscuration are correlated in local, UV-bright starburst galaxies; the recipe of Calzetti (1997b) can then be used to predict the total amount of energy absorbed by dust, provided that the value  $R'_V=4.05$  (instead of 4.88, see Calzetti 1997b) is used in conjunction with the reddening curve. The

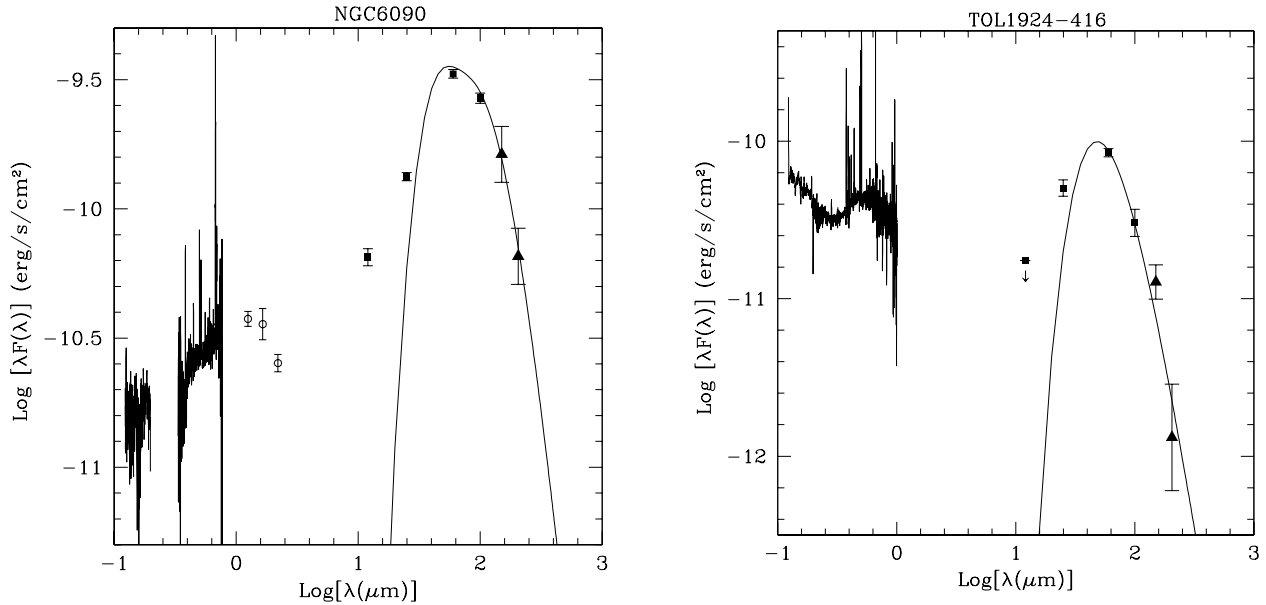


Figure 3: The UV-optical-nearIR-farIR SEDs of two low-redshift starburst galaxies: the FIR-luminous NGC6090 (left panel) and the Blue Compact Dwarf Tol1924–416 (right panel). UV-optical spectrophotometry is shown as a continuous line in the wavelength range  $0.12\text{--}1.0\ \mu\text{m}$ , nearIR photometry as empty circles, IRAS data as filled squares, and ISO measurements as filled triangles (Calzetti et al. 1999). Upper limits have downward arrows. For NGC6090, the far-IR data are fit by two modified Planck functions with temperatures  $T_1=49\ \text{K}$  and  $T_2=23\ \text{K}$  and, for Tol1924–416, by a single modified Planck function with temperature  $T=50\ \text{K}$ . The fits are shown as solid curves. The emissivity of the dust is taken to be  $\nu^2$ .

predicted values match the observed far-IR emission of individual cases within a factor 2, but, when averaged over a large sample of galaxies, the predicted value matches the median of the observations within 20%.

As said above, the Lyman-break galaxies resemble local UV-bright starbursts; the reddening/obscuration recipe derived for the latter objects should then be applicable to the former ones to obtain predictions on the total far-IR dust emission (Meurer et al. 1999, Calzetti et al. 1999). However, whether a high-redshift galaxy will be detectable or not with the currently available instrumentation depends not only on the total far-IR flux but also on the dust SED. SCUBA at the JCMT has been proven very effective at detecting galaxies at cosmological distances, especially in the sensitive  $850\ \mu\text{m}$  band (e.g., Hughes et al. 1998, Eales et al. 1998, Blain et al. 1999, Lilly et al. 1999, Barger et al. 1999). For a  $z\sim 3$  galaxy, this band probes the restframe  $\sim 210\ \mu\text{m}$  emission, longward of the peak of the dust SED, usually located between  $60$  and  $100\ \mu\text{m}$  in actively star-forming galaxies (e.g., Helou 1986, see Figure 3). The fraction of light emitted at  $200\ \mu\text{m}$  relative to the total far-IR dust luminosity varies by at least one order of magnitude among starburst galaxies. An example is shown in Figure 3, where the UV-to-far-IR SEDs of two local starburst galaxies are reported. In the FIR-luminous galaxy NGC6090,  $\lambda F(\lambda)_{205}/F_{far-IR}=0.12$ , where  $\lambda F(\lambda)_{205}$  is the energy coming out in the  $205\ \mu\text{m}$  ISO band and  $F_{far-IR}$  is the total far-IR dust emission; in the Blue Compact Dwarf galaxy Tol1924–416,  $\lambda F(\lambda)_{205}/F_{far-IR}=0.013$ , about a factor 10 smaller than in NGC6090 (Calzetti et al. 1999). Indeed, Tol1924–416 has hotter dust than NGC6090. If the far-IR SED of each galaxy is fitted with two modified Planck functions at different temperatures, the two temperatures have values  $T_1=49\ \text{K}$  and  $T_2=23\ \text{K}$  for NGC6090, but only one temperature value,  $T=50\ \text{K}$ , can be derived for Tol1924–416. This galaxy is missing the cooler dust component (a result independent of the adopted dust emissivity index).

Why is Tol1924–416 warmer than NGC6090? One possible reason is the difference in the total dust content of the two galaxies: the Blue Compact Dwarf is about 10 times more metal poor than the FIR-luminous NGC6090, implying that, for the same gas content, the dust column density is also about 10 times smaller. Dust self-shielding is less efficient in the metal-poor object and the dust will tend to be hotter (Mezger, Mathis & Panagia 1982).

Detecting dust emission in just one band thus leaves the ambiguity of the actual SED to be adopted to derive the total far-IR emission from the galaxy. Observations at sub-mm and mm wavelengths in multiple bands will be needed to actually understand the physical characteristics of the far-IR emission from high-redshift galaxies (e.g., is the dust in UV-bright Lyman-break galaxies hotter than in local galaxies?), and pin down the total amount of dust contained in the distant progenitors of present-day galaxies.

## 4 The Evolution of the Star Formation Rate Density

In recent years, a wealth of data have become available on the luminosity density of the Universe at a variety of wavelengths and redshifts. One of the scopes of these measurements is to derive the evolution of the SFRD of the Universe (see the pioneering work of Madau et al. 1996), as a way to characterize the global evolution of the stellar populations in galaxies.

A number of uncertainties affect the conversion of a luminosity density into a SFRD, in addition to the problems usually encountered in statistical studies, such as volume corrections, luminosity selections, etc. A thorough discussion of all the uncertainties is given by D. Schaerer (these Proceedings); a few of those relevant to the present discussion are mentioned here. For UV measurements, the largest uncertainty is represented by dust corrections; as seen in the previous sections, presence of dust in galaxies can absorb between 50% and 80% of the UV light. The next largest uncertainty at all wavelengths is the stellar IMF, which is poorly known especially at the low mass end, where most of the stellar mass is contained; this carries a factor 2–3 uncertainty in the conversion of a luminosity density into a SFRD. For measurements longward of  $\sim 2,000 \text{ \AA}$  (excluding recombination lines), another source of uncertainty is the galaxy star formation history: the longer a galaxy has been forming stars, the more intermediate/low mass stars have been accumulating, and the more flux is accumulating in the integrated light at redder wavelengths. Variations of the star formation history between galaxies induces uncertainties up to  $\sim 30\text{--}50\%$  in the SFRD derived from, e.g., data at  $2800 \text{ \AA}$ .

Figure 4 reports UV,  $H\alpha$ , and mid/far-IR luminosity density data at a variety of redshifts, collected from the literature; the luminosities have been converted to SFRDs assuming a Salpeter IMF with mass range  $0.35\text{--}100 M_{\odot}$  and a 1 Gyr constant star formation stellar population. The data form a ‘progression’ from UV to  $H\alpha$  to mid/far-IR in the left panel of Figure 4: the longer the wavelength, the higher, on average, the estimated SFRD. This is consistent with presence of dust obscuration in the galaxies. The right panel of Figure 4 reports the same data after dust correction: the spread at each redshift value is now smaller than in the left panel. The UV and  $H\alpha$  data have been corrected according to the results reported in the previous sections, while the mid/far-IR data have not been corrected. For  $z < 1$ , I have assumed that the corrections to apply to the UV data are the same as those derived for the  $z \sim 1$  galaxies. In addition, among the  $H\alpha$  luminosity points, only the data of Glazebrook et al. (1999) and Yan et al. (1999) have been corrected (the point from Gronwall 1998 has been already corrected by the author).

The dust-corrected data of Figure 4 are consistent with the SFRD being roughly constant between  $z \sim 1.2\text{--}1.4$  and  $z \sim 4$  and about 5 times larger than what directly measured from UV data. Between  $z \sim 1.2$  and  $z = 0$ , the SFRD decreases by a factor  $\sim 10$  (Lilly et al. 1996) and

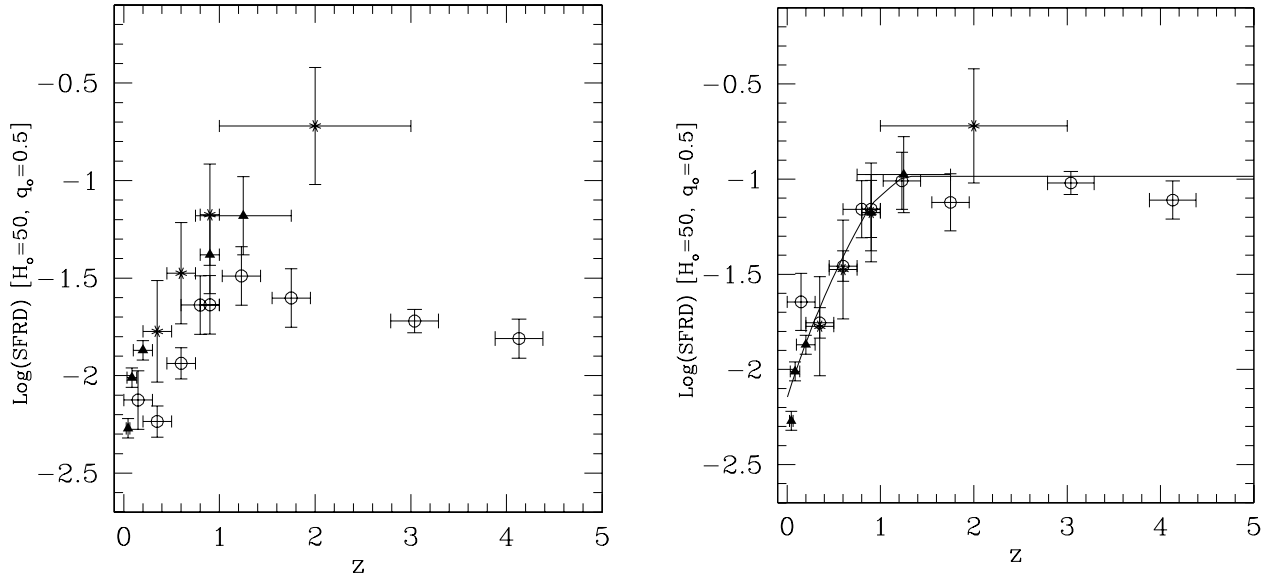


Figure 4: The average star formation rate density in the Universe, SFRD, in  $M_{\odot} \text{ yr}^{-1} \text{ Mpc}^{-3}$  as a function of redshift, before (left panel) and after (right panel) correction for the effects of dust obscuration. Empty circles indicate restframe UV data at  $2800 \text{ \AA}$  (for  $z < 2$ , Lilly et al. 1996, Connolly et al. 1997) and at  $1700 \text{ \AA}$  (for  $z > 2$ , Steidel et al. 1999). Filled triangles mark the position of the  $H\alpha$  measurements (Gallego et al. 1995, Gronwall 1998, Tresse & Maddox 1998, Glazebrook et al. 1999, Yan et al. 1999). Asterisks mark the position of mid/far-IR data, from ISO ( $z < 1$ , Flores et al. 1998) and from SCUBA (see text for references).  $1 \sigma$  error bars are reported for all the data. The continuous line in the right panel represents one of the models for the evolution of the SFRD of the Universe from Calzetti & Heckman (1999, their Model 3).

is about 3 times larger than what inferred from the UV measurements. The comparison with one of the SFRD evolution models of Calzetti & Heckman (1999) highlights the trend just described. This implies that up to  $\sim 20\%$  of all the stars were formed before  $z=3$  and up to  $\sim 60\%$  before  $z \sim 1.2$ . Excess of metal production has often been put forward as an argument against large SFRD values at high redshifts; however, gas inflows/outflows in/out of galaxies can completely offset the problem, as the excess metals get dispersed into the IGM. One of the advantages of a high SFRD at  $z > 2$  is the ability to reproduce the Cosmic Infrared Background observed by COBE (see, for the observations, Fixsen et al. 1998, Hauser et al. 1998, and, for the models, Calzetti & Heckman 1999, Pei et al. 1999).

In conclusion, dust obscuration affects the observed light from high redshift galaxies, with flux reductions up to a factor 5 when targeting the restframe UV. This happens even and especially at high redshift. Although common wisdom would suggest that metallicities are low in the young Universe, gas column densities are high so dust opacity can be high; in addition the observer optical waveband corresponds to restframe far-UV, a wavelength region strongly affected by dust obscuration.

One question which has not been answered yet, but is very important for measuring the SFRD at high redshift, is the relationship between the UV-bright Lyman-break galaxies and the FIR-bright SCUBA galaxies. In Figure 4 the data from the Lyman-break galaxies and from the SCUBA galaxies are used as if originating from the same objects (although at different wavelengths). However, if the two type of galaxies are complementary, rather than overlapping, populations, their contributions to the SFRD would sum up, rather than average together, increasing the high redshift SFRD by another factor  $\sim 2$ . In this case, a problem may arise,

as the global SFR would be large enough to deplete galaxies of their gas content before  $z=0$ . Clearly, the nature of the two galaxy populations need to be addressed, to understand whether such a problem may exist.

## 5 Acknowledgements

I would like to thank C. Leitherer (STScI) for a critical reading of the manuscript and the Organizing Committee of the XXXIVth Recontres de Moriond for inviting me to this very interesting meeting and for financially supporting my stay at Les Arcs. Part of this trip has been supported by the STScI Director Discretionary Research Funds.

## References

- [1] Barger, A.J., Cowie, L.L., Smail, I., Ivison, R.J., Blain, A.W., & Kneib, J.-P. 1999, *Astrophys. J. in press*, (astroph/9903142)
- [2] Baugh, C.M., Cole, S., Frenk, C.S., & Lacey, C.G. 1998, *Astrophys. J.* **498**, 504
- [3] Blain, A.W., Kneib, J.-P., Ivison, R.J., & Smail, I. 1999, *Astrophys. J.* **512**, L87
- [4] Calzetti, D. 1997a, *Astron. J.* **113**, 162
- [5] Calzetti, D. 1997b, in *The Ultraviolet Universe at Low and High Redshift: Probing the Progress of Galaxy Evolution*, eds. W.H. Waller, M.N. Fanelli, J.E. Hollis & A.C. Danks, AIP Conf. Proc. 408 (Woodbury: AIP), 403
- [6] Calzetti, D., Armus, L., Bohlin, R.C., Kinney, A.L., Koornneef, J., Storchi-Bergmann, T., & Wyse, R.F.G. 1999, *in prep.*
- [7] Calzetti, D., Bohlin, R.C., Kinney, A.L., Storchi-Bergmann, T., & Heckman, T.M. 1995, *Astrophys. J.* **443**, 136
- [8] Calzetti, D., & Heckman, T.M. 1999, *Astrophys. J. in press*, (astroph/9811099)
- [9] Calzetti, D., Kinney, A.L., & Storchi-Bergmann, T. 1994, *Astrophys. J.* **429**, 582
- [10] Connolly, A.J., Szalay, A.S., Dickinson, M., Subbarao, M.U., & Brunner, R.J. 1997, *Astrophys. J.* **486**, L11
- [11] Dickinson, M. 1998, in *The Hubble Deep Field*, STScI May Symposium, eds. M. Livio, S.M. Fall, & P. Madau, (Cambridge: CUP), 219
- [12] Eales, S., Lilly, S., Gear, W., Dunne, L., Bond, J.R., Hammer, F., Le Fèvre, O., & Crampton, D. 1999, *Astrophys. J.* **515**, 518
- [13] Fixsen, D.J., Dwek, E., Mather, J.C., Bennett, C.L., Shafer, R.A. 1998, *Astrophys. J.* **508**, 123
- [14] Flores, H., Hammer, F., Thuan, T.X., Césarski, C., Desert, F.X., Omont, A., Lilly, S.J., Eales, S., Crampton, D., & Le Fèvre, O., 1999 *Astrophys. J.* **517**, 148
- [15] Gallego, J., Zamorano, J., Aragon-Salamanca, A., & Rego, M. 1995, *Astrophys. J.* **455**, L1
- [16] Glazebrook, K., Blake, C., Economou, F., Lilly, S., & Colless, M. 1999, *MNRAS in press*, (astroph/9808276)
- [17] Gordon, K.A., Calzetti, D., & Witt, A.N. 1997, *Astrophys. J.* **487**, 625

- [18] Gronwall, C., 1998, in *Dwarf Galaxies and Cosmology, the XXXIIIrd Recontres de Moriond*, eds. T.X. Thuan, C. Balkowski, V. Cayatte & J. Tran Thanh Van (Gif-sur-Yvette: Editions Frontières), *in press* (astroph/9806240)
- [19] Hauser, M.G., Arendt, R.G., Kelsall, T., Dwek, E., et al. *Astrophys. J.* **508**, 25
- [20] Helou, G. 1986, *Astrophys. J.* **311**, L33
- [21] Hughes, D., Serjeant, S., Dunlop, J., Rowan-Robinson, M., Blain, A., Mann, R.G., Ivison, R., Peacock, J., Efstathiou, A., Gear, W., Oliver, S., Lawrence, A., Longair, M., Goldschmidt, P., & Jenness, T. 1998, *Nature* 394 24
- [22] Leitherer, C., & Heckman, T.M. 1995, *Astrophys. J. Suppl. Ser.* **96**, 9
- [23] Lilly, S.J., Eales, S.A., Gear, W.K.P., Hammer, F., Le Fevre, O., Crampton, D., Bond, J.R., & Dunne, L. 1999, *Astrophys. J. in press*, (astroph/9901047)
- [24] Lilly, S.J., Le Fèvre, O., Hammer, F. & Crampton, D. 1996, *Astrophys. J.* **460**, L1
- [25] Madau, P., Ferguson, H.C., Dickinson, M.E., Giavalisco, M., Steidel, C.C., & Fruchter, A. 1996, *MNRAS* **283**, 1388
- [26] Meurer, G. R., Heckman, T.M., & Calzetti, D. 1999, *Astrophys. J. in press*, (astroph/9812360)
- [27] Meurer, G. R., Heckman, T.M., Lehnert, M.D., Leitherer, C., & Lowenthal, J. 1997, *Astron. J.* **114**, 54
- [28] Mezger, P.G., Mathis, J.S., & Panagia, N. 1982, *Astr. Astrophys.* **105**, 372
- [29] Pei, Y.C., Fall, S.M., & Hauser, M.G. 1999, *Astrophys. J. in press*, (astroph/9812182)
- [30] Pettini, M., Kellogg, M., Steidel, C.C., Dickinson, M., Adelberger, K.L., & Giavalisco, M. 1998, *Astrophys. J.* **508**, 539
- [31] Steidel, C.C., Giavalisco, M., Pettini, M., Dickinson, M., & Adelberger, K.L. 1996, *Astrophys. J.* **462**, L17
- [32] Steidel, C.C., Adelberger, K. L., Giavalisco, M., Dickinson, M., & Pettini, M. 1999, *Astrophys. J. in press*, (astroph/9811399)
- [33] Tresse, L., & Maddox, S.J. 1998, *Astrophys. J.* **495**, 691
- [34] Witt, A.N., Thronson, H.A., & Capuano, J.M. 1992, *Astrophys. J.* **393**, 611
- [35] Yan, L., McCarthy, P.J., Freudling, W., Teplitz, H.I., Malumuth, E.M., Weymann, R.J., & Malkan, M.A. 1999, *Astrophys. J. Letter in press*, (astroph/9904427)
- [36] Young, J.S., Xie, S., Kenney, J.D.P., & Rice, W.L. 1989, *Astrophys. J. Suppl. Ser.* **70**, 699